THERMAL-IR DETECTION OF OPTICAL OUTFLOW SOURCES IN OMC1 SOUTH[1]

Nathan Smith[2,3], John Bally[3], Ralph Y. Shuping[4], Mark Morris[4], and Thomas L. Hayward[5]

ABSTRACT

We present the first thermal-infrared imaging photometry for several embedded sources in the OMC1 South cloud core in the Orion nebula, and propose that some of these drive optical Herbig-Haro jets emerging from the region. Thermal-infrared images at 8.8 and 11.7 μm obtained at Gemini South show a handful of sources in OMC1-S with no visual-wavelength counterparts, although a few can be seen in recent near-infrared data. For the three brightest mid-infrared sources, we also present 18.75 μm photometry obtained with the Keck telescope. The most prominent blueshifted outflows in the Orion nebula at visual wavelengths such as HH 202, HH 203/204, HH 529, and HH 269 all originate from OMC1-S. The brightest infrared source in OMC1-S at 11.7 μm is located at the base of the prominent jet that powers HH 202 and is likely to be the sought-after driver of this outflow. The second brightest infrared source is located at the base of the HH 529 jet. We consider the possibility that HH 203/204 and HH 269 trace parts of a single bent outflow from the third-brightest infrared source. While there may be some lingering ambiguity about which infrared stars drive specific jets, there is now a sufficient number of embedded sources to plausibly account for the multiple outflows from OMC1-S.

Subject headings: H II regions — ISM: Herbig-Haro objects — ISM: individual (Orion nebula) — ISM: jets and outflows — stars: formation — stars: pre–main-sequence

1. INTRODUCTION

Two luminous star-forming cloud cores lurk immediately behind the main ionization front of the Orion nebula and the Trapezium cluster: the $\sim 10^5$ L$_\odot$ BN/KL nebula in the OMC1 cloud core and the $\sim 10^4$ L$_\odot$ OMC1 South region, both of which are hidden at visual wavelengths. The BN/KL nebula is a bright and complex region associated with a spectacular wide-angle bipolar outflow, powerful masers, and ultra-compact H II regions, and has been studied in great detail at infrared (IR) wavelengths (e.g., Allen & Burton 1993; Gezari et al. 1998; Shuping et al. 2004; Kaifu et al. 2000; see O'Dell 2001 for a recent review).

Were it not upstaged by its spectacular northern neighbor, OMC1-S would be the most luminous star-forming core and the most dramatic outflow source in the Orion molecular cloud complex. OMC1-S resides

---

[2]Hubble Fellow; nathans@casa.colorado.edu

[3]Center for Astrophysics and Space Astronomy, University of Colorado, 389 UCB, Boulder, CO 80309

[4]Division of Astronomy and Astrophysics, University of California at Los Angeles, Los Angeles, CA 90095

[5]Gemini Observatory, Association of Universities for Research in Astronomy, Inc., Casilla 603, La Serena, Chile

within a visually dark and protruding region of the Orion nebula $\sim 60''$ southwest of the Trapezium (Wen & O'Dell 1995). First noted as an extended far-infrared source (Keene, Hillenbrand, & Whitcomb 1982), it harbors the luminous far-IR/sub-mm source FIR4 (Mezger et al. 1990), the dense molecular condensation CS3 (Mundy et al. 1986), several compact water masers (Gaume et al. 1998), and at least two bipolar molecular outflows with nearly orthogonal axes (Ziurys, Wilson, & Mauersberger 1990; Schmid-Burgk et al. 1990; Rodriguez-Franco et al. 1999a, 1999b). Additionally, Bally, O'Dell, & McCaughrean (2000) noted that at least a half-dozen highly collimated Herbig-Haro (HH) outflows emerge from within OMC1 South, giving rise to shocks best seen in *Hubble Space Telescope* (*HST*) or Fabry-Perot images (see O'Dell et al. 1997; O'Dell & Doi 2003; Rosado et al. 2001). Proper motions of these HH objects determined by *HST* indicate dynamical ages of several hundred to a few thousand years (Bally et al. 2000; O'Dell & Doi 2003). Gaume et al. (1998) discovered near-IR point sources within $\sim 15''$ of FIR4, offering a possible source for the embedded CO jet discovered by Schmid-Burgk et al. (1990). However, no compact IR sources have yet been reported as plausible drivers for most of the numerous optically-visible HH jets that emerge from OMC1-S.

In this Letter we report the discovery of several thermal-IR point sources in the OMC1-S cloud core. We postulate that some of these drive optical HH outflows from the region, since they are located at the expected origin points of the jets deduced from proper-motions and from new Fabry-Perot images.

2. OBSERVATIONS

2.1. Thermal-IR Images

Images of the Orion nebula at 8.8 μm ($\Delta\lambda$=8.35-9.13 μm) and 11.7 μm ($\Delta\lambda$=11.09-12.22 μm) were obtained on 2004 Jan 26 and 25, respectively, using T-ReCS on Gemini South. T-ReCS is the facility mid-IR imager and spectrograph with a 320×240 pixel Si:As IBC array, a pixel scale on the 8m Gemini South telescope of $0\rlap{.}''089$, and a resulting field-of-view of $28\rlap{.}''5 \times 21\rlap{.}''4$. The observations were taken with a $15''$ east-west chop throw. Since the throw is much smaller than the extent of the nebula, we took a series of east-west scans while chopping, starting on relatively blank sky to the west, and stepping by $15''$ per pointing. To define the reference sky to subtract from each position, we took the minimum of two frames on either side of the position of interest. This allowed effective removal of point sources in the reference sky frames, but some nebular emission persisted where both adjacent pointings contained diffuse emission at the same position on the array. This technique worked sufficiently well in the OMC1-South region, but degraded the image quality somewhat because of small pointing errors in the off-source beam. Individual sky-subtracted frames were combined to make a larger mosaic image, using point sources in each frame for spatial alignment.

Figure 1a shows a portion of the resulting 11.7 μm mosaic image for the region of the OMC1-South molecular cloud core southwest of the Trapezium. Table 1 lists J2000 coordinates for IR sources in this field, numbered 1–11, as well as point-source photometry at 8.8 and 11.7 μm measured in a $0\rlap{.}''9$ radius synthetic aperture. These coordinates were measured with a 2-D radial profile fit relative to θ^1Ori C (included in the surveyed region but not shown in Fig. 1a), assuming a position for θ^1Ori C of α_{2000}=$5^{\mathrm{h}}35^{\mathrm{m}}16\rlap{.}^{\mathrm{s}}46$, δ_{2000}=$-5°23'23\rlap{.}''0$ (McCaughrean & Stauffer 1994). The relative positional uncertainty is better than 1 pixel ($\sim 0\rlap{.}''09$). Flux densities in Table 1 were measured with respect to the secondary standard star HD 32887, adopting the values tabulated by Cohen et al. (1999). Point-source sensitivity was approximately 8.3 and 10.5 mJy (1σ) at 8.8 and 11.7 μm, respectively, although uncertainty for the brighter sources is dominated by ±5–10% uncertainty in the calibration stars.

In addition, we have obtained images of the OMC1-S region at 18.75 μm ($\Delta\lambda = 18.3 - 19.2$) using the Long Wavelength Spectrometer (LWS) at the Keck Observatory on 2002 Nov 16. LWS employs a 128×128 As:Si BIB array with a pixel scale of 0$\farcs$081, yielding a 10$\farcs$2×10$\farcs$2 field of view (Jones & Puetter 1993). Weather conditions were moderately stable during the second half of the night, when OMC1-S was imaged. We employed a standard mid-IR chop-nod technique, with the chopping secondary driven at 2 and 5 Hz with 20$''$ and 10$''$ E–W throws, respectively. The standard star β And was also observed throughout the night for PSF determination and flux calibration. Flux densities for sources 1–3 at 18.75 μm are listed in Table 1. Sources 1 and 2 were measured with a 15-pixel (1$\farcs$21) radius aperture; while Source 3 was measured using an 8-pixel (0$\farcs$648) aperture to reduce the contribution of faint diffuse emission. Each source was observed in several different frames and the frame-to-frame variation (which we attribute to weather) was ~5%. The total uncertainty for sources 1 and 3 is $\lesssim$7%, while for source 2 it is 16% due to the uncertain local background level. Because of local diffuse emission surrounding source 2, the reported flux density is aperture dependent.

Sources 7-9 and 11 have visual-wavelength counterparts, appearing stellar or unresolved in *HST* images (O'Dell & Wong 1996). The fact that these "naked" stars have detectable thermal-IR emission suggests that they have retained dusty disks not resolved by *HST*. Sources 1-6 and 10 are invisible at optical wavelengths and are most likely embedded protostellar sources, although the position of source 10 lies outside the OMC1-S cloud core. This is the first reported measurement of these sources at thermal-IR wavelengths. Of these, only sources 4 and 5 have been reported previously in the near-IR (sources B and C; Gaume et al. 1998).[1]

Thermal-IR spectral energy distributions (SEDs) for sources 1-6 are shown in Figure 1b. Blackbody curves are shown for a rough comparison. It is clear that sources 1 and 2 are more luminous and more deeply embedded than sources B and C. Sources 1, 2, 3, and 6 are good candidates for deeply embedded outflow sources. Of course, the data shown in Figure 1 provide underestimates of the true bolometric luminosities, since dust having a broad range of temperatures may emit at wavelengths not observed here. Furthermore, the far-IR luminosity of the region (~10^4 L$_\odot$; Johnstone & Bally 1999) is much higher than the sum of the mid-IR luminosities inferred from our data. Also note that the blackbody curves in Figure 1 and the color temperatures and luminosities in Table 1 do not account for silicate absorption or reddening.

2.2. Visual Wavelength Fabry-Perot Images

In order to determine whether our IR sources are associated with HH flows, we compare our T-ReCS data with Fabry-Perot images obtained by Bally et al. (2004) using the Multi-Object Spectrograph/Fabry-Perot at the f/8 Cassegrain focus of the 3.6-meter Canada-France-Hawaii Telescope (CFHT). For details of the observations and an analysis of the results, see Bally et al. (2001, 2004). The rectified data cube has a velocity resolution of about 13 km s^{-1}, a pixel scale of 0$\farcs$44 pixel^{-1}, and a free spectral range of 392 km s^{-1}.

Figure 2 shows an image extracted from a portion of the [O III] λ5007 data cube of the central Orion nebula, color-coded with velocity, such that features near the systemic velocity are red, low-velocity blueshifted features are green, and fast blueshifted features are blue. Figure 2 also illustrates the positions of the embedded IR sources 1–6 in OMC1-S from Figure 1 and Table 1.

[1]Source TCC009 of McCaughrean & Stauffer (1994) is within 1$''$ of our source 3, but it is not clear that these are the same source because more recent data give the impression that the near-IR source may be a reflection nebula. A close inspection of the near-IR Subaru image of Orion by Kaifu et al. (2000) reveals that all mid-IR sources except 3 and 6 have perceptible 2 μm counterparts, although these were unremarked by Kaifu et al.

3. OUTFLOWS AND THEIR SOURCES

We have detected several closely-spaced thermal-IR sources in OMC1 South, while Bally et al. (2000) noted at least six optical HH jets that emerge from sources hidden within the cloud core (HH 202, HH 529, HH 203/204, HH 528, HH 530, and HH 269). HH 625, an additional flow found by O'Dell & Doi (2003), and at least two molecular outflows, also originate in OMC1-S. Here we discuss possible associations between these various outflow systems and the embedded IR sources that we have detected.

HH 202: This is the most prominent HH object in Figure 2, and it was one of the first in the Orion nebula to be recognized as such (also named M42-HH2; Cantó et al. 1980; Meaburn 1986). FP data (Fig. 2; O'Dell et al. 1997; Rosado et al. 2001; Bally et al. 2004) show a highly collimated jet emerging from OMC1-S and extending to the brightest part of HH 202. Source 1 lies almost exactly along the presumed axis of the HH 202 jet within 5″ of where the irradiated jet body emerges from the cloud, and it is the best candidate for the driver of the HH202 jet. If so, then proper motions (O'Dell & Doi 2003) would indicate a dynamical age of 2300±500 yr. While we cannot positively rule out the possibility that either source 2 or 3 drives the HH202 jet, we note that source 2 probably drives HH529 and source 3 may drive both HH203/204 and HH269 (see below). To assign either source 2 or 3 the additional burden of driving HH202 (the most prominent jet in the Orion nebula) seems less straightforward than attributing it to the most luminous IR source in OMC1-South (source 1), which is not a plausible driving source for any other blueshifted HH jet.

HH 529: The HH 529 jet extends east from an embedded source in OMC1-S at position angle PA ≈ 100°. As shown in Figure 2, IR source 2 is located exactly along the jet axis a few arcseconds west of where the optical jet originates. No other IR source lies along the jet axis, so source 2 is the best candidate for the origin point of HH529. O'Dell & Doi (2003) deduced the expected location of the driving source responsible for HH 529 from proper motions to be at $5^h35^m14\overset{s}{.}56$, $-5°23'54''$, where no optical source is seen. This location is within 3″ of source 2. If source 2 is the origin of HH 529, then the jet has a dynamical age of 1100±150 yr. O'Dell & Doi also suggested that this "optical outflow source" (OOS) is responsible for driving the HH 269 jet (the presumed counterjet to HH 529), and perhaps HH 202, HH 528, and HH 203/204.

HH 203/204 and HH 269: The HH 203/204 shocks trace a blueshifted outflow extending southeast of OMC1-S at PA≃135°. Unlike HH 202 and 529, this jet cannot be traced all the way back to OMC1-S; it becomes invisible about 1′ southeast of this core. The jet beam also seems to point somewhat east of OMC1-S. Rosado et al. (2001) proposed that HH 203/204 and HH 202 trace opposite lobes of a bipolar outflow emerging form OMC1-South. However, both lobes exhibit large blueshifts, requiring a C-shaped or bent outflow structure. Although Bally et al. (2000, 2001) report several bent HH flows in the Orion nebula, all exhibit bends in the plane of the sky, consistent with deflection by a wind emerging from the nebular core. If HH 203/204 and 269 originate from OMC1-South, deflection by a stellar wind from the Trapezium stars or the plasma flowing way from the nebula's main ionization front would deflect the flow toward the southwest.

We propose that instead of being the counterlobe to HH 202, the HH 203/204 pair is the deflected counterlobe to HH 269. An arc extending through these objects passes through IR source 3, located several arc seconds south of source 2. Therefore, it may be the case that this object powers a bipolar outflow deflected toward the southwest and toward our line of sight. The morphology, radial velocity, and proper motions of HH 203/204 support this hypothesis, as discussed further by Bally et al. (2004).

HH 528: We have argued above that HH 203/204 is not the counterjet to HH 202 as suggested intially by Rosado et al. — but if HH 202 does have a visual-wavelength counterjet (instead of one that simply burrows

into the background molecular cloud and disappears), then the best candidate may be HH 528. HH 528 has a low-velocity redshift (Bally et al. 2004), and may be lost in the bright emission from the ionization front if it is moving nearly in the plane of the sky. The position angle of HH 528 is $140°$–$150°$ with respect to source 1, 2, or 3, which makes it a plausible companion to the HH 202 jet at P.A.$\simeq 320°$. However, the dynamical age of ~ 5000 yr (Bally et al. 2000) still makes it somewhat problematic to link HH 528 and the younger HH 202 jet as part of the same bipolar flow, unless HH 528 has been decelerated. Alternatively, HH 528 could potentially be associated with the fast molecular outflow source and HH 625, discussed below.

Embedded molecular outflows, HH 530, and HH 625: Two different molecular outflows have been detected in OMC1-S; one fast and one relatively slow, with orthogonal axes. The fast (~ 110 km s^{-1}) bipolar CO jet is oriented southeast/northwest (Rodriguez-Franco et al. 1999b). Rodriguez-Franco et al.'s expected position for this fast molecular outflow source (labeled "FMOS" in Fig. 1) is coincident with the near-IR source "A" (Gaume et al. 1998). We detect no thermal-IR source at this position, but given the spatial resolution of the original data, source B could easily be the culprit as well. In fact, in an earlier analysis of the same data, Rodriguez-Franco et al. (1999a) gave a different point of origin for the FMOS located several arcseconds to the southeast. O'Dell & Doi (2003) suggested that HH 625 is where the blueshifted component of this flow breaks out into the H II region. Since OMC1-S protrudes from the main ionization front of the Orion nebula (Wen & O'Dell 1995), it is conceivable that HH 528 could be where the redshifted part of this same bipolar flow escapes from the molecular cloud.

The second embedded molecular outflow is a highly-collimated, low-velocity redshifted flow toward the southwest from OMC1-S, with a poorly-collimated blueshifted counterflow (Schmid-Burgk et al. 1990). The origin of this jet is usually attributed to FIR4 or CS3 (Mezger et al. 1990; Mundy 1986). Bally et al. (2000) proposed that HH 530 (see Fig. 2) is an optical counterpart to the low-velocity CO jet, and proper motions indicate an origin near FIR4+CS3 as well. Since one of the most important outflow sources in OMC1-S is apparently located in the vicinity of FIR4+CS3, it is interesting that we detect no thermal-IR source there at 8.8 or 11.7 μm. This driving source must be more deeply embedded than the others in OMC1-S, and higher-resolution observations at longer IR, submm, and radio wavelengths are needed to measure its position and constrain its physical properties.

In summary, we have discovered several embedded thermal-IR sources in OMC1-S, some of which we identify as likely driving sources for HH jets seen at visual wavelengths. This overal picture of several individual sources driving independent highly-collimated outflows with different dynamical ages is distinct from the high-luminosity BN/KL outflow 90″ to the north, which is a wide angle outflow that probably originated from a single explosive event, forming multiple HH objects at the tips of the outflowing fingers.

REFERENCES

Allen, D.A., & Burton, M.G. 1993, Nature, 353, 54

Bally, J., O'Dell, C.R., & McCaughrean, M.J. 2000, AJ, 119, 2919

Bally, J., Johnstone, D., Joncas, G., Reipurth, B., & Mallén-Ornelas, G. 2001, AJ, 122, 1508

Bally, J., Johnstone, D., and Joncas, G. 2004, AJ, in preparation

Cantó, J., Goudis, C., Johnson, P.G., & Meaburn, J. 1980, A&A, 85, 128

Cohen, M., Walker, R.G., Carter, B., Hammersley, R., Kidger, M., & Nogushi, K. 1999, AJ, 117, 1864

Gaume, R.A., Wilson, T.L., Vrba, F.J., Johnston, K.J., & Schmid-Burgk, J. 1998, ApJ, 493, 940

Gezari, D.Y., Backman, D.E., & Werner, M.W. 1998, ApJ, 509, 283

Johnstone, D., & Bally, J. 1999, ApJ, 510, L49

Jones, B., & Puetter, R.C. 1993, in Proc. SPIE Vol. 1946, Infrared Detectors and Instrumentation, A.M. Fowler, Ed., 610–621

Kaifu, N., et al. 2000, PASJ, 52, 1

Keene, J., Hildebrand, R. H., & Whitcomb, S. E. 1982, ApJ, 252, L11

McCaughrean, M.J., & Stauffer, J.R. 1994, AJ, 108, 1382

Meaburn, J 1986, A&A, 164, 358

Mezger, P.G., Wink, J.E., & Zylka, R. 1990, A&A, 228, 95

Mundy, L.G., Scoville, N.Z., Bååth, L.B., Masson, C.R., & Woody, D.P. 1986, ApJ, 304, L51

O'Dell, C.R. 2001, ARAA, 39, 99

O'Dell, C.R., & Doi, T. 2003, AJ, 125, 277 (Erratum: 2003, AJ, 125, 2753)

O'Dell, C.R., Hartigan, P., Bally, J., & Morse, J. 1997, AJ, 104, 2016

O'Dell, C.R., & Wong, S.K. 1996, AJ, 111, 846

Rodriguez-Franco, A., Martin-Pintado, J., & Wilson, T.L. 1999a, A&A, 344, L57

Rodriguez-Franco, A., Martin-Pintado, J., & Wilson, T.L. 1999b, A&A, 351, 1103

Rosado, M., de la Fuente, E., Arias, L., Raga, A., & Le Coarer, E. 2001, AJ, 122, 1928

Schmidt-Burgk, J., Güsten, R., Mauersberger, R., Schulz, A., & Wilson, T.L. 1990, ApJ, 362, L25

Shuping et al. 2004, AJ, in press (July 2004)

Wen, Z., & O'Dell, C.R. 1995, ApJ, 438, 784

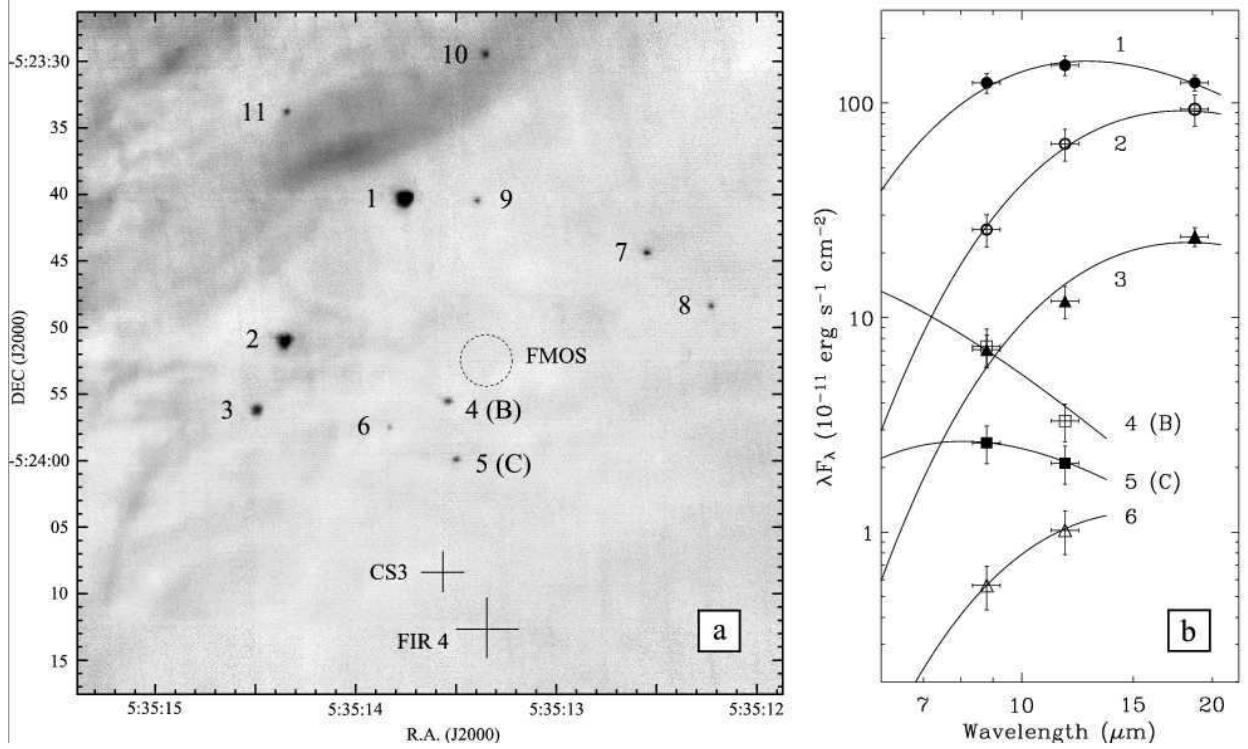Ziurys, L. M., Wilson, T. L., & Mauersberger, R. 1990, ApJ, 356, 25

Fig. 1.— (a) 11.7 μm image mosaic of the OMC1-S region. Sources 1-11 are listed in Table 1. Reported positions of FIR4 (Mezger et al. 1990), CS3 (Mundy et al. 1986), and the approximate position of the fast molecular outflow source (FMOS; Rodriguez-Franco et al. 1999b) are also indicated. The position of source A (Gaume et al. 1998) is located within the FMOS circle. (b) Spectral energy distributions for embedded sources in OMC1-S. Fluxes are taken from Table 1. Representative Planck functions are drawn through the data points, with corresponding temperatures and luminosities given in Table 1.
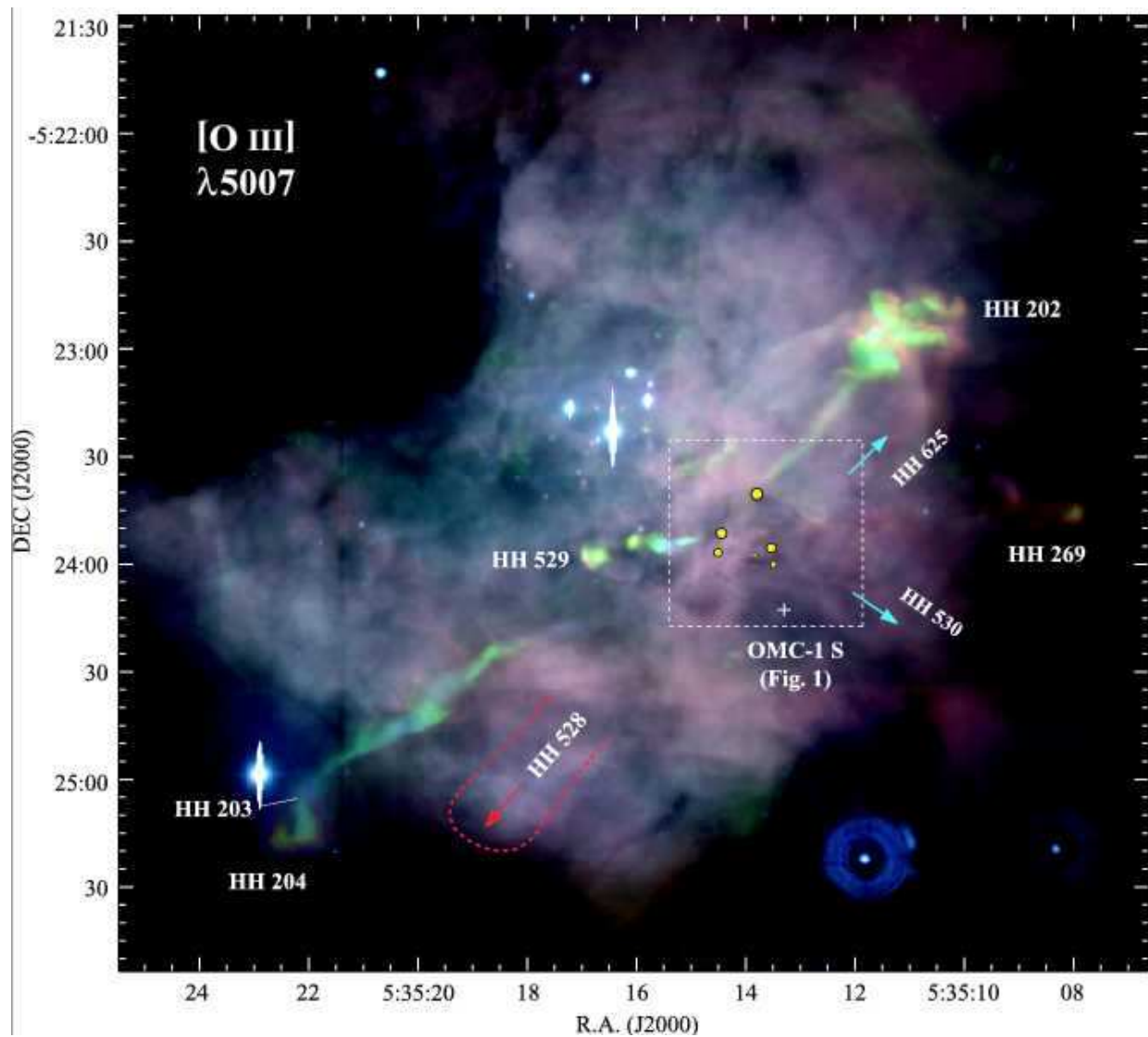
Fig. 2.— Fabry-Perot image of the Orion nebula in [O III] $\lambda5007$ (see Bally et al. 2004), color-coded by velocity so that features near the systemic velocity appear red, low-velocity blueshifts appear green, and fast blueshifted features are blue. Positions of embedded IR sources 1–6 from Fig. 1 in OMC1-S are marked with yellow dots, and major HH jets are labeled.

Table 1.   IR Point Sources in OMC1-S

IRS	Name	R.A. (J2000)	DEC (J2000)	8.8 μm F_ν(Jy)	11.7 μm F_ν(Jy)	18.8 μm F_ν(Jy)	T_C (K)	L_{IR} ($L_\odot$)
1	138-340	5:35:13.80	-5:23:40.3	3.6	6.4	7.8	290	13.6
2	144-351	5:35:14.40	-5:23:51.0	0.75	2.5	5.8	205	7.9
3	145-356	5:35:14.54	-5:23:56.2	0.21	0.46	1.5	200	1.9
4	B	5:35:13.58	-5:23:55.5	0.22	0.13	$\cdots$	980	1.5
5	C	5:35:13.55	-5:23:59.9	0.077	0.082	$\cdots$	460	$(0.2)^{\mathrm{a}}$
6	139-357	5:35:13.88	-5:23:57.4	0.017	0.040	$\cdots$	230	0.1
7	126-344	5:35:12.60	-5:23:44.4	0.21	0.22	$\cdots$	$\cdots$	$\cdots$
8	122-348	5:35:12.28	-5:23:48.4	0.10	0.11	$\cdots$	$\cdots$	$\cdots$
9	134-340	5:35:13.44	-5:23:40.4	0.070	0.096	$\cdots$	$\cdots$	$\cdots$
10	134-330	5:35:13.40	-5:23:29.5	0.18	0.19	$\cdots$	$\cdots$	$\cdots$
11	144-334	5:35:14.39	-5:23:33.8	0.23	0.28	$\cdots$	$\cdots$	$\cdots$

[a]This mid-IR luminosity is an underestimate for the total luminosity of C, as near-IR data (Gaume et al. 1998) combined with our data would indicate a value closer to 1 $L_\odot$.